Ab initio study of collective excitations in a disparate mass molten salt

Taras Bryk and Ivan Klevets

Citation: J. Chem. Phys. **137**, 224508 (2012); doi: 10.1063/1.4770269
View online: http://dx.doi.org/10.1063/1.4770269
View Table of Contents: http://jcp.aip.org/resource/1/JCPSA6/v137/i22
Published by the American Institute of Physics.

Ab initio study of collective excitations in a disparate mass molten salt

Taras Bryk[1,2] and Ivan Klevets[1]
[1]*Institute for Condensed Matter Physics of the National Academy of Sciences of Ukraine, 1 Svientsitskii Street, UA-79011 Lviv, Ukraine*
[2]*Institute of Applied Mathematics and Fundamental Sciences, National Polytechnic University of Lviv, UA-79013 Lviv, Ukraine*

(Received 27 August 2012; accepted 26 November 2012; published online 14 December 2012)

Ab initio molecular dynamics simulations and the approach of generalized collective modes are applied for calculations of spectra of longitudinal and transverse collective excitations in molten LiBr. Dispersion and damping of low- and high-frequency branches of collective excitations as well as wave-number dependent relaxing modes were calculated. The main mode contributions to partial, total, and concentration dynamic structure factors were estimated in a wide region of wave numbers. A role of polarization effects is discussed from comparison of mode contributions to concentration dynamic structure factors calculated for molten LiBr from *ab initio* and classical rigid ion simulations. © *2012 American Institute of Physics*. [http://dx.doi.org/10.1063/1.4770269]

I. INTRODUCTION

Binary liquids with disparate masses reveal very interesting features of collective dynamics.[1] Large mass difference causes a manifestation of high-frequency collective excitations as a side peak of the partial dynamic structure factor of light component that was observed in molecular dynamics (MD) computer simulations of the liquid binary alloy Li_4Pb.[2] The dispersion of the high-frequency branch obtained from the side peak positions revealing a high slope in the long-wavelength region was ascribed to so-called "fast sound" excitations that correspond to propagating modes over the light component on the background of atoms of heavy component. The inelastic neutron scattering experiments performed for molten Li_4Pb and Li_4Tl[3] supported the MD findings on existence of the high-frequency excitations. The "fast sound" excitations were also observed in MD simulations of rare-gas mixtures with disparate masses.[4,5] There were a few attempts of analytical theory for "fast sound" based on mode coupling theory[2] and memory function approach for binary liquids.[6,7] However only the most advanced theoretical approach for exploration of dynamics in liquids known as the method of generalized collective modes (GCM)[8–10] was able to correctly explain the origin of the "fast sound" observation in the disparate mass binary liquids.[11,12]

Collective dynamics in molten salts reveals special features in comparison with atomic dynamics of liquid mixtures and metallic alloys.[13,14] We would like to remind that hydrodynamic theory, which in fact is based on local conservation laws, leads to analytical expressions for dynamic structure factors $S(k, \omega)$, where k and ω denote wave-number and frequency, with contributions from solely most slow dynamic processes having their lifetimes $\propto k^{-2}$ in the long-wavelength limit. And analytical expressions for density-density time correlation functions in the long-wavelength limit give evidence that the slow hydrodynamic processes with the lifetimes $\propto k^{-2}$ have independent on k amplitudes (weights) of their contributions,[14] while all non-hydrodynamic processes[15] have short lifetime and vanishing amplitudes at least as $\propto k^2$ for $k \to 0$. In general the relation between the lifetimes of relaxation processes and their contributions to dynamic structure factors beyond hydrodynamic region is very sophisticated, although for pure liquids there are available analytical expressions obtained in viscoelastic approximation.[16]

However it follows from the hydrodynamic theory of molten salts[17,18] that due to local electroneutrality condition the relaxation process connected with ionic conductivity has the finite lifetime in the long-wavelength limit in contrast to liquid mixtures where the similar relaxation process connected with mutual diffusivity shows the $\propto k^{-2}$ dependence of its lifetime. Therefore for simple liquid mixtures the concentration dynamic structure factor $S_{cc}(k, \omega)$ does not show any side peak for small wave numbers while in molten salts, i.e., binary liquids with long-range Coulomb interaction even in the limit $k \to 0$ there exists a non-zero contribution of $S_{cc}(k, \omega)$ coming from non-hydrodynamic optic modes.[19] The issue of non-hydrodynamic (not predicted by hydrodynamic theory) optic-like modes and their manifestation in dynamic structure factors is extremely interesting. For long time it was believed that optic modes cannot exist in liquids. However computer simulations, performed on molten salts[20,21] and binary liquid alloys[22] clearly showed the existence of high-frequency collective excitations caused by concentration (charge for ionic systems) fluctuations. Recently there appeared even reports on observation of the optic modes in molten NaCl and NaI[23] in inelastic X-ray scattering experiments (IXS). The theory for optic modes had to be based on generalized hydrodynamics, and for the case of molten salts it was constructed using the GCM approach,[19] whereas for liquid mixtures it was reported for transverse dynamics in Ref. 24, and for longitudinal case in Ref. 25.

The role of mass asymmetry in single-particle dynamics of molten salts was studied before. The mass dependence of the single-particle velocity autocorrelation functions was reported in Refs. 26 and 27. However by date the collective

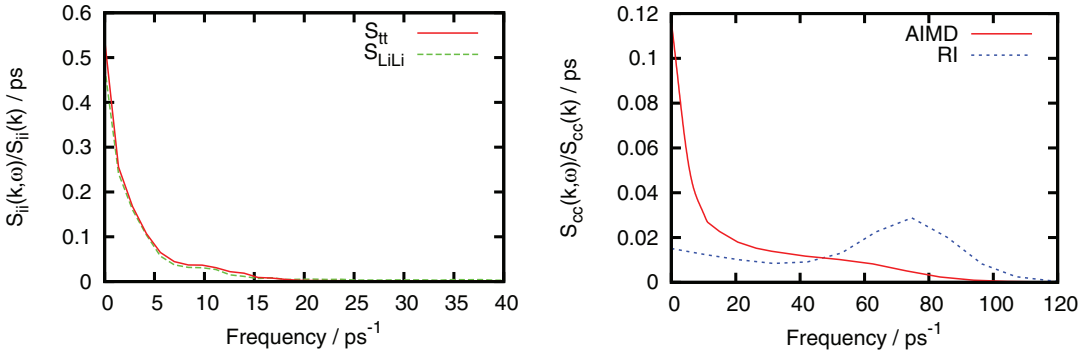

FIG. 1. Total $S_{tt}(k)$ and partial Li-Li dynamic structure factor $S_{\mathrm{LiLi}}(k)$ (left frame) and concentration dynamic structure factor $S_{cc}(k)$ (right frame, solid line) for $k = 0.543$ Å^{-1} obtained from *ab initio* MD simulations of LiBr at 905 K. Concentration dynamic structure factor at $k = 0.514$ Å^{-1} obtained within the rigid ion (RI) model in classical MD simulations is shown in the right frame by dotted line.

dynamics of solely molten salts with relatively small mass ratio was studied. Moreover, the *ab initio* molecular dynamics (AIMD) studies of collective dynamics are very rare in the literature because the numerical estimation of dispersion of collective excitations from peak positions of corresponding current spectral functions results in huge error bars and there is a need in computational methodology to be able to predict more precisely the frequencies of collective excitations. In this sense the GCM approach is namely such a methodology that permits reliable analysis of time correlation functions derived in *ab initio* simulations. Previously the classical[28] and *ab initio* simulations[29,30] with GCM analysis were applied to calculations of dispersion of longitudinal and transverse collective excitations in molten NaCl and NaI. The GCM modes in two more molten salts LiF and RbF were reported in Ref. 31. All these molten salts have the mass ratio of heavy to light components $R = m_h/m_l$ between 1.54 (NaCl) and 5.52 (NaI) whereas our task is to study the collective excitations in a realistic molten salt with much larger mass ratio of components. For this purpose we have chosen the molten LiBr with the mass ratio $R = 11.51$.

Besides, an interesting issue is to estimate collective modes that contribute to the dynamic structure factors in the molten salts with disparate masses beyond the hydrodynamic regime. Polarization effects should play an important role in the mode contributions.[32] This can be illustrated by Fig. 1 where we show the partial $S_{\mathrm{LiLi}}(k, \omega)$ and total $S_{tt}(k, \omega)$ dynamic structure factors (left frame) and concentration dynamic structure factor $S_{cc}(k, \omega)$, obtained from AIMD data for wave-number $k = 0.543$ Å^{-1}. The formers are very similar that is typical for the systems with long-range interaction, for which in the long-wavelength region the partial and total dynamic and static structure factors coincide. One can see in Fig. 1 that the $S_{\mathrm{LiLi}}(k, \omega)$ and $S_{tt}(k, \omega)$ have a shoulder at rather low frequency $\sim$10 ps^{-1}. However the concentration dynamic structure factors obtained from AIMD and classical rigid ion (RI) simulations show essentially different strengths of relaxation and propagating processes. For $S_{cc}(k, \omega)$ calculated in *ab initio* MD one observes a strong central peak and a shoulder at frequency $\sim$60 ps^{-1}, while $S_{cc}^{RI}(k, \omega)$ calculated with the classical RI model reveals a strong side peak at $\sim$80 ps^{-1} and rather small central peak. Similar observations from classical MD simulations of molten salts with different screening properties were reported by Giaquinta *et al.*[33] This issue should be studied in more detail using the GCM methodology.

Hence, this study of collective dynamics in molten LiBr has two aims: (i) calculate by means of *ab initio* molecular dynamics simulations and GCM approach the dispersion of acoustic and optic branches and estimate the role of polarization effects on longitudinal and transverse optic branches by comparing them with the corresponding results of classical rigid ion simulations, and, (ii) to evaluate the contributions from collective excitations and relaxation processes to dynamic structure factors and their changes due to polarization effects. In particular this second part should shed light on the possibility to observe "fast sound" in disparate mass molten salts.

The remaining paper has the following structure: in Sec. II, we give details of our methodology of calculations of collective excitations from *ab initio* MD simulations, Sec. III contains results on static structure factors, spectra of propagating and relaxing modes, mode contributions to dynamic structure factors and Sec. IV presents the conclusions of this study.

II. METHODOLOGY

The *ab initio* simulation of the molten salt LiBr at temperature 905 K was performed with a collection of 150 particles in a cubic box with the boxlength 16.3508 Å. The initial configuration was taken from RI classical simulations with Tosi-Fumi potentials for LiBr.[26] The equilibration in *ab initio* simulations was performed in *NVT* ensemble over 5 ps. The time step in simulations was 1.5 fs, and the production runs lasted up to 35.5 ps, that permitted to have 23 700 configurations for statistical averages of static and dynamic quantities.

The electron-ion interactions were represented by PAW potentials.[34] The PAW methodology in contrast to regular pseudopotential approach permits to obtain correct atomic-like oscillating behaviour of wave functions in the atomic core and hence all the total energy calculations are performed with true (not pseudo-) electron density.[34,35] The generalized gradient approximation in Perdew-Burke-Ernzerhof version[36] was applied in order to account for exchange-correlation effects in strongly non-uniform electron density of molten LiBr.

The cut-off energy for expansion of wave functions in plane waves was 216.26 eV. The electron density was constructed using a single Γ point in the Brillouin zone that was justified by quite large box size.

In order to compare the *ab initio* and rigid ion results we performed classical simulations at the same temperature and density for a system of 500 particles. The short-range part of effective potentials[26] was cut at 12.2 Å, and the long-range part was treated by the standard Ewald summation. The time step for classical simulations was the same as in AIMD.

We stress that the two types of simulations, *ab initio* and classical rigid ion ones, were needed in order to calculate the dispersion of optic branch without any assumption on effective interactions in molten salts[37] and estimate the role of polarization effects. For precise IXS experiments it is extremely important to know the frequencies of the non-hydrodynamic optic branch. The location of optic branch especially in the long-wavelength region is extremely sensitive to different levels of account for polarization effects in effective force fields of classical molecular dynamics as it was shown in Ref. 37. Therefore we aimed to compare the dispersion of longitudinal and transverse optic branches for two limiting cases: full account for polarization effects within the *ab initio* MD and no polarization effects for rigid ion simulations.

For the purpose of GCM analysis we saved the trajectories, velocities of particles as well as forces acting on them. Forty five wave numbers were sampled, and all the corresponding wave vectors with different directions but the same absolute value were used for additional averages of static and dynamic quantities. The smallest wave-number for our system was $k_{min} = 0.384$ Å^{-1}. For each wave-number we analyzed the longitudinal and transverse time correlation functions with 6-variable and 4-variable dynamic models, respectively. The spectrum of collective excitations was obtained as a wave-number dependence of imaginary parts of complex eigenvalues of generalized hydrodynamic matrix $\mathbf{T}(k)$, whereas the real parts of complex eigenvalues represented damping of propagating modes. Purely real eigenvalues of $\mathbf{T}(k)$ represented the relaxing modes having the sense of their wave-number dependent inverse relaxation time as follows from the GCM expression for time correlation functions.[9,15] All the matrix elements of $\mathbf{T}(k)$ were calculated directly from MD data avoiding any fit. The expressions for matrix elements of $\mathbf{T}(k)$ can be found elsewhere.[9,38]

The longitudinal dynamics of LiBr was analyzed within the six-variable viscoelastic set of dynamic variables:

$$\mathbf{A}^{(6)}(k,t) = \{n_{\mathrm{Li}}(k,t), n_{\mathrm{Br}}(k,t), J^L_{\mathrm{Li}}(k,t), J^L_{\mathrm{Br}}(k,t), \dot{J}^L_{\mathrm{Li}}(k,t), \dot{J}^L_{\mathrm{Br}}(k,t)\}, \quad (1)$$

where $n_i(k,t)$ are the Fourier-components of partial densities of particles, $J^L_i(k,t)$ - of the longitudinal components of partial mass-currents, and $\dot{J}^L_i(k,t)$ are the extended dynamic variables represented via first time derivative of partial currents. The time evolution of these six dynamic variables was obtained in *ab initio* MD simulations and used for calculations of the 6 × 6 generalized hydrodynamic matrix for longitudinal dynamics. For the transverse dynamics the same level of treatment of short-time processes is provided by the following transverse four-variable set:

$$\mathbf{A}^{(4T)}(k,t) = \{J^T_{\mathrm{Li}}(k,t), J^T_{\mathrm{Br}}(k,t), \dot{J}^T_{\mathrm{Li}}(k,t), \dot{J}^T_{\mathrm{Br}}(k,t)\} \quad (2)$$

with $J^T_i(k,t)$ being the transverse components of partial mass-currents, and $\dot{J}^T_i(k,t)$ - their first time derivatives. The eigenvalues and associated eigenvectors obtained for the generalized hydrodynamic matrices constructed on sets (1) and (2) were analyzed for each of forty five wave numbers sampled.

III. RESULTS AND DISCUSSION

A. Structure factors

In Fig. 2 we show the Bhatia-Thornton total $S_{tt}(k)$ (left frame) and concentration $S_{cc}(k)$ (right frame) static structure factors obtained from *ab initio* and classical RI simulations. Typically as for molten salts there is rather small first peak of $S_{tt}(k)$ located at $k \sim 1.9$ Å^{-1}. The results on $S_{tt}(k)$ from AIMD and classical RI simulations are in reasonable agreement. For concentration static structure factor the agreement between two types of simulations is very good. The main peak of $S_{cc}(k)$ is well pronounced, for RI model it has even larger amplitude. For our task of estimation of the role of polarization effects in collective dynamics the most interesting is the long-wavelength behaviour of $S_{cc}(k)$ that according to Ref. 13 behaves as

$$S_{cc}(k)\Big|_{k\to 0} \sim \frac{\varepsilon_\infty k_B T}{4\pi n e^2} k^2, \quad (3)$$

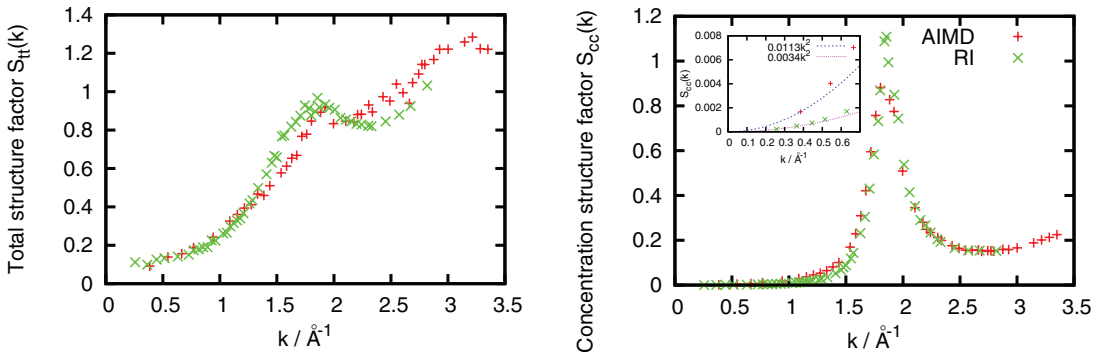

FIG. 2. Bhatia-Thornton static structure factors $S_{tt}(k)$ (left frame) and $S_{cc}(k)$ (right frame) for LiBr at 905 K, obtained from *ab initio* MD (symbols plus) and classical simulations with rigid ion model (symbols cross). The inset shows the long-wavelength asymptotes of both $S_{cc}(k)$.

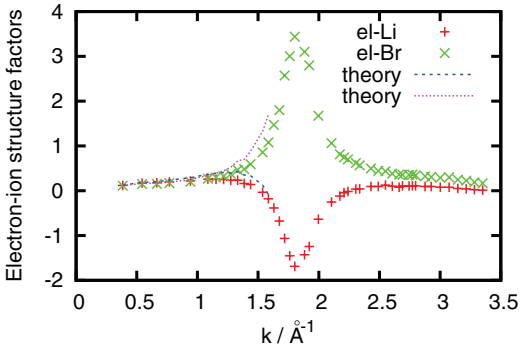

FIG. 3. Partial electron-ion structure factors $S_{\mathrm{Li}-el}(k)$ and $S_{\mathrm{Br}-el}(k)$ calculated directly from *ab initio* molecular dynamics. The lines represent analytical expressions for long-wavelength behaviour of partial electron-ion structure factors.[40,41]

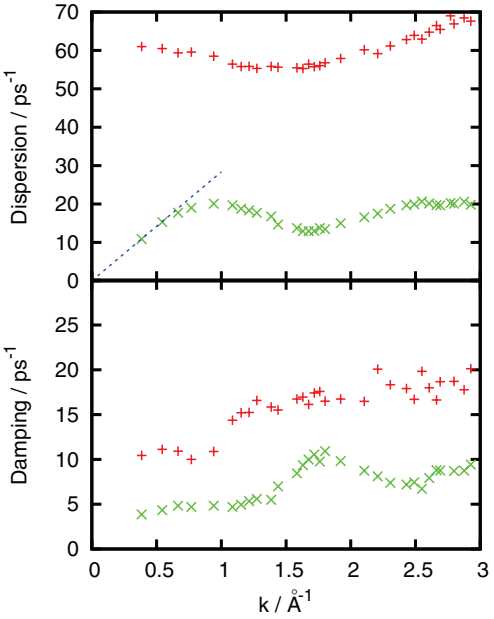

FIG. 4. Dispersion and damping of longitudinal collective excitations as obtained from the fit-free GCM calculations based on the six-variable (1) dynamic model for longitudinal dynamics. The straight line corresponds to a linear dispersion law with the high-frequency speed of sound c_∞. The cross/plus symbols show the dispersion and damping of low/high frequency branch.

where n is the numerical density, ε_∞ – the high-frequency dielectric permittivity, e – elementary charge. For RI classical model there is obviously $\varepsilon_\infty = 1$ because the electronic shells do not polarize for rigid ions. Therefore the results of $S_{cc}(k)$ from AIMD always have higher values in the long-wavelength region. Since all the other parameters in (3) were identical in both simulations, the ratio of asymptotes shown in inset of Fig. 2 permits to estimate the high-frequency dielectric permittivity $\varepsilon_\infty = 3.32$ for molten LiBr at 905 K. This value is in good agreement with the value of high-frequency dielectric permittivity 3.17 for LiBr crystal.[39]

Another possibility that give AIMD simulations is in estimation of electron-ion correlations. In Fig. 3 we show the partial electron-ion structure factors compared in the long-wavelength region with the theoretical expressions.[40,41] One can see that the agreement between theory and simulations is good in the long-wavelength region where the theoretical expressions are valid. Note that these results are the first electron-ion structure factors reported for molten salts and obtained directly from *ab initio* simulations. Before only for network-forming binary liquids $GeSe_4$,[42] SiO_2, and $GeSe_2$[43] similar calculations were performed. Interestingly that in the region of the main peak of $S_{cc}(k)$ both electron-ion structure factors have their peaks, however with opposite signs, although for $k \to 0$ both $S_{i-el}(k)$ should be identical. Perhaps the different signs in the region $k \sim 1.8$ Å^{-1} indicate excess of electrons for negative Br ions and lack of electrons for positive Li ions, because we observed similar behaviour of $S_{i-el}(k)$ in molten salts RbF, NaI, and LiF.[44]

B. Dispersion of collective excitations

Spectra of longitudinal collective excitations are shown in Fig. 4. Among the six eigenvalues obtained within the dynamic model (1) we have two pairs of complex-conjugated ones

$$z_\alpha = \sigma_\alpha(k) \pm i\omega_\alpha(k), \quad \alpha = 1, 2$$

where the imaginary parts correspond to dispersion and real parts – to damping of propagating modes. The two branches of collective excitations are well separated in frequency and from their dispersion one can easily estimate the origin of each branch. The low-frequency branch in the long-wavelength region shows a linear with wave-number dispersion and corresponds to longitudinal acoustic (LA) excitations. Our estimate for the apparent speed of sound at the smallest wave-number is $c = 2822$ m/s. The damping of acoustic modes shown by cross symbols in bottom frame of Fig. 4 gives evidence that the smallest wave-number sampled in AIMD is in fact beyond the hydrodynamic regime, because in the limit $k \to 0$ the damping of acoustic modes in hydrodynamic regime should be proportional to k^2. To reach the hydrodynamic regime in molten salts the simulations with at least 1000 particles are needed. However the GCM predictions of features of collective dynamics in molten salts beyond the hydrodynamic regime are very important for IXS experiments. Recently the GCM predictions on so-called "positive" dispersion of acoustic excitations[45] were successfully supported by IXS experiments on different liquids.[46,47]

The high-frequency branch in Fig. 4 corresponds to longitudinal optic (LO) modes and it tends to a frequency $\sim$61 ps^{-1} in the long-wavelength limit. Typically as for non-hydrodynamic excitations the damping of optic modes tends to a finite non-zero value in the long-wavelength limit. This means that the optic-like excitations do not survive on macroscopic time scales in comparison with hydrodynamic LA modes. With increase of wave numbers the frequency of LO branch shows a decay up to $k \sim 1.5$ Å^{-1} followed by increase of frequency in the short-wavelength region as this should be for both branches in the Gaussian regime ($k \to \infty$ limit) with a higher slope of increase of frequency for the high-frequency branch, because in the large-k region that branch corresponds to partial dynamics of light particles. The damping of the

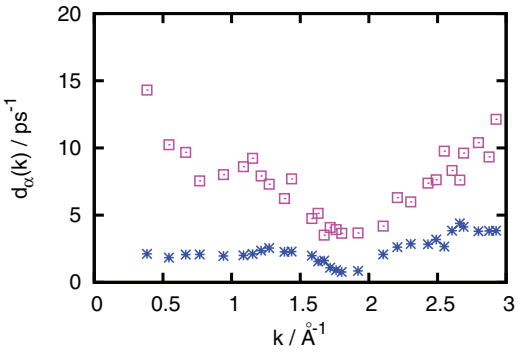

FIG. 5. Wave-number dependence of real eigenvalues, representing relaxing modes in longitudinal dynamics. Star symbols - structural relaxation, boxes - relaxation connected with ionic conductivity.

high-frequency branch is larger in the entire wave-number region than the damping of the low-frequency branch, although a strong increase of damping of the low-frequency modes is observed at $k \sim 1.75$ Å^{-1}. This region of wave numbers corresponds to the minimum of the corresponding dispersion curve shown in the top frame of Fig. 4 and the observed effect of de Gennes slowing down of density fluctuations.[14]

Purely real eigenvalues correspond to the relaxing modes in the liquid system. In order to discriminate between complex eigenvalues (propagating modes) and purely real ones (relaxing modes) in GCM expressions we will mark the latters as $d_\alpha(k)$, $\alpha = 1, 2$. The $d_\alpha(k)$ have the meaning of wave-number dependent inverse relaxation times of corresponding processes. In Fig. 5 the wave-number dependent relaxing modes obtained for molten LiBr within the six-variable dynamic model (1) are shown. The origin of these relaxing modes will be clearly seen in Subsection III C where the contributions from propagating and relaxing modes to total and concentration dynamic structure factors are reported. Thermal effects are not studied within the dynamic model (1) because in molten salts the ratio of specific heats γ is close to unity that justifies the applied viscoelastic approach. Besides, in our previous GCM study of collective dynamics of molten salts[19] we compared the results obtained for collective modes with the full account for coupling with thermal processes and without it (viscoelastic models) and showed perfect applicability of the viscoelastic models for description of dynamics of molten salts. Therefore both relaxing modes $d_\alpha(k)$, obtained within the viscoelastic dynamic model (1), are of non-thermal origin. The more slow relaxing mode (shown with stars in Fig. 5 is the well known non-hydrodynamic structural relaxation $d_{str}(k)$, whereas the hydrodynamic relaxation process connected with ionic conductivity σ is shown in Fig. 5 by open boxes. In the long-wavelength limit this relaxing mode tends to the following value:[17]

$$d_{cond}(k)\Big|_{k\to 0} = \frac{4\pi\sigma}{\varepsilon_\infty}. \tag{4}$$

One can see that in region $k \sim 1.8$ Å^{-1} both relaxing modes have minima of their wave-number dependence, that corresponds to increase of their relaxation times in the region of de Gennes slowing down of density fluctuations.[48]

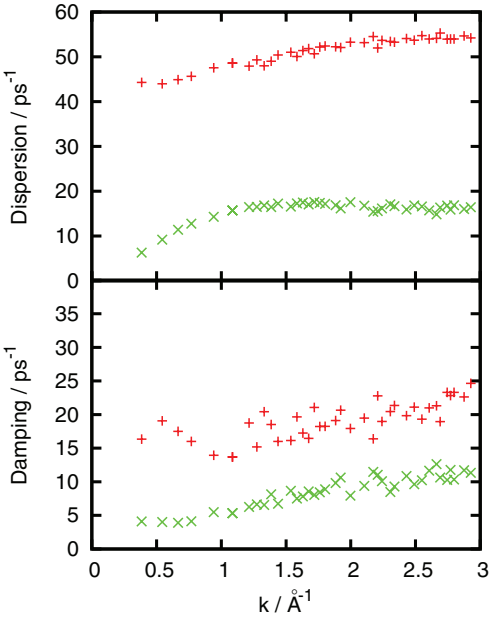

FIG. 6. Dispersion and damping of transverse collective excitations as obtained from the fit-free GCM calculations based on the four-variable (2) dynamic model for transverse dynamics. The cross/plus symbols show the dispersion and damping of low/high frequency branch.

Dispersion and damping of transverse collective modes obtained within the dynamic model (2) are shown in Fig. 6. Even for the smallest wave-number we obtained two complex-conjugated pairs of eigenvalues that gives evidence on smaller than 0.384 Å^{-1} width of the propagation gap for shear waves in molten LiBr. The propagation gap for shear waves defines in fact the region of viscoelastic transition for transverse dynamics. In fact existing propagating transverse modes at the smallest wave-number give evidence that at the spatial scale $l \sim 2\pi/k_{min}$ the dynamics in molten LiBr is defined by elastic mechanism. The high frequency branch of transverse optic (TO) excitations tends in the long-wavelength limit to a frequency ~44.5 ps^{-1}, indicating that the LO-TO gap between long-wavelength longitudinal and transverse optic modes in LiBr is 16.5 ps^{-1}.

The role of polarization effects in collective dynamics of molten salts can be estimated from comparison of the dispersion of optic branches calculated from *ab initio* and classical RI MD simulations. In Fig. 7 the dispersion of longitudinal

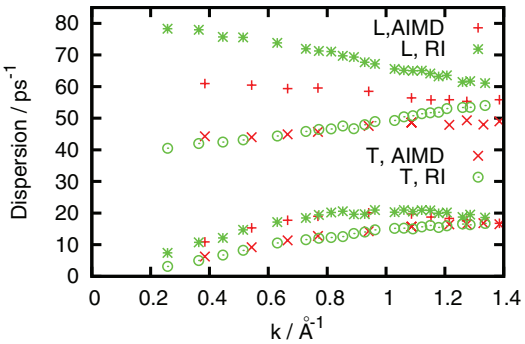

FIG. 7. Dispersion of longitudinal (L) and transverse (T) collective excitations in comparison with results of the rigid ion (RI) classical simulations.

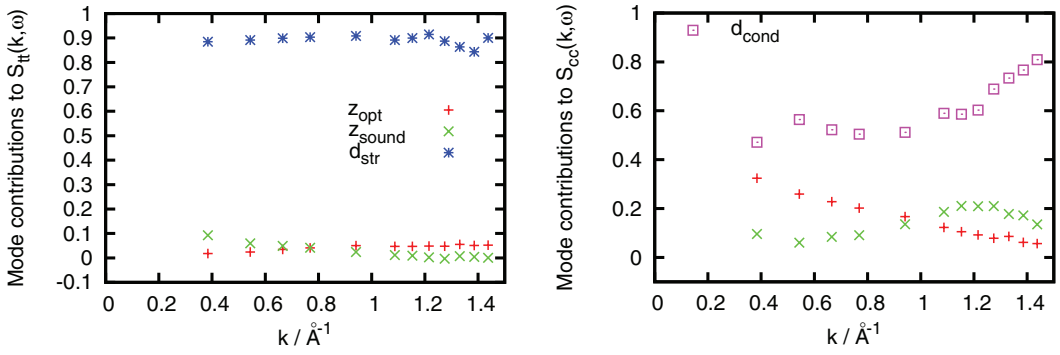

FIG. 8. Mode contributions to Bhatia-Thornton dynamic structure factors obtained from *ab initio* MD simulations of molten LiBr at 905 K. Left frame: $A_{tt}^{str}(k)$ and $B_{tt}^{\alpha}(k)$ in $S_{tt}(k,\omega)$. Right frame: $A_{cc}^{cond}(k)$ and $B_{cc}^{\alpha}(k)$ in $S_{cc}(k,\omega)$.

and transverse collective excitations from both simulations is shown. The low-frequency branches both in L and T case coincide in AIMD and RI simulations. The essential difference is mainly observed for the longitudinal optic (LO) branch. The softening of the LO branch due to polarization of the electron shells of ions is about 18 ps^{-1}, i.e., the frequency of the long-wavelength LO mode in RI model ~80 ps^{-1} is reducing to the value of LO mode from AIMD. The softening of the LO excitations due to polarization effects was suggested to lead to a reduction of LO-TO gap by $\sqrt{\varepsilon_\infty}$ times.[49] Indeed, our results show, that the reduction of the LO-TO gap in Fig. 7 is about 1.82 times, that is very close to the square root of our estimated value of the high-frequency dielectric permittivity ε_∞.

C. Contributions from collective modes to dynamic structure factors

A great advantage of the GCM approach is in the possibility to decompose any dynamic structure factor of interest into separable mode contributions. In Ref. 16 it was suggested to represent the amplitudes of mode contributions as wave-number-dependent real functions instead of complex ones. For the six-variable dynamic model (1) one obtains for time correlation functions the following GCM expression in a form that is a generalization of hydrodynamic expressions on the case of additional non-hydrodynamic contributions:

$$\frac{F_{ij}^{(6)}(k,t)}{F_{ij}(k)} = A_{ij}^{cond}(k)e^{-d_{cond}(k)t} + A_{ij}^{str}(k)e^{-d_{str}(k)t} + \sum_{\alpha=1}^{2}\left[B_{ij}^{\alpha}(k)\cos(\omega_\alpha(k)t) + D_{ij}^{\alpha}(k)\sin(\omega_\alpha(k)t)\right]e^{-\sigma_\alpha(k)t},\ i,j = t,c,\mathrm{Li},\mathrm{Br}. \tag{5}$$

The corresponding dynamic structure factors read

$$\frac{S_{ij}^{(6)}(k,\omega)}{S_{ij}(k)} = A_{ij}^{cond}(k)\frac{2d_{cond}(k)}{\omega^2+d_{cond}^2(k)} + A_{ij}^{str}(k)\frac{2d_{str}(k)}{\omega^2+d_{str}^2(k)} + \sum_{\alpha=1}^{2}\left[B_{ij}^{\alpha}(k)\frac{\sigma_\alpha(k)}{[\omega\pm\omega_\alpha(k)]^2+\sigma_\alpha^2(k)} \pm D_{ij}^{\alpha}(k)\frac{\omega\pm\omega_\alpha(k)}{[\omega\pm\omega_\alpha(k)]^2+\sigma_\alpha^2(k)}\right]. \tag{6}$$

In (6) the amplitudes of mode contributions (or mode strengths as called in Ref. 13) $A_{ij}^{\alpha}(k)$ represent weights of relaxation processes contributing to the central peak of $S_{ij}(k,\omega)$, whereas $B_{ij}^{\alpha}(k)$ and $D_{ij}^{\alpha}(k)$ reflect symmetric (Lorentzian) and asymmetric (non-Lorentzian) contributions to the side peaks.

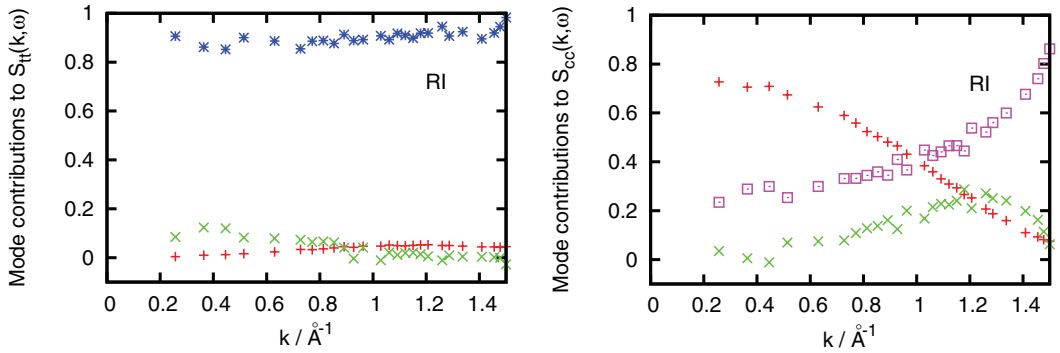

FIG. 9. Mode contributions to Bhatia-Thornton dynamic structure factors obtained from classical MD simulations with rigid ion model of molten LiBr at 905 K. Left frame: $A_{tt}^{str}(k)$ and $B_{tt}^{\alpha}(k)$ in $S_{tt}(k,\omega)$. Right frame: $A_{cc}^{cond}(k)$ and $B_{cc}^{\alpha}(k)$ in $S_{cc}(k,\omega)$.

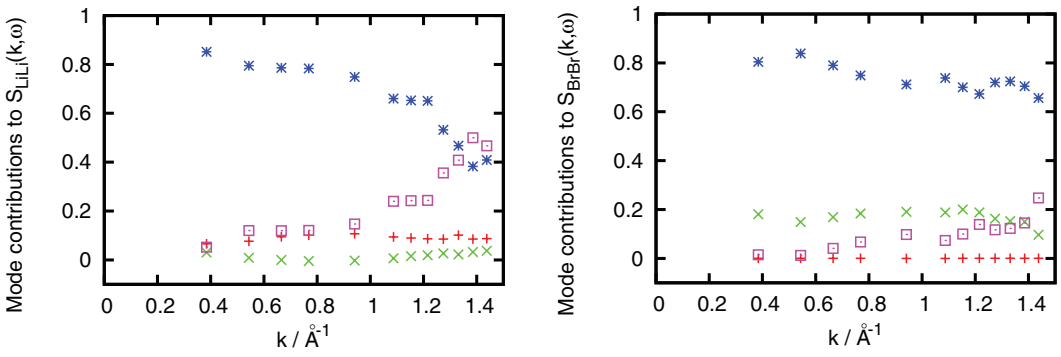

FIG. 10. Mode contributions to partial dynamic structure factors obtained from *ab initio* MD simulations of molten LiBr at 905 K. Left frame: $A^{str}_{\mathrm{LiLi}}(k)$, $A^{cond}_{\mathrm{LiLi}}(k)$, and $B^{\alpha}_{\mathrm{LiLi}}(k)$ in $S_{\mathrm{LiLi}}(k,\omega)$. Right frame: $A^{str}_{\mathrm{BrBr}}(k)$, $A^{cond}_{\mathrm{BrBr}}(k)$, and $B^{\alpha}_{\mathrm{BrBr}}(k)$ in $S_{\mathrm{BrBr}}(k,\omega)$. Symbols correspond to the modes of the same origin as in Figure 9.

In Fig. 8 we show the most important mode contributions to normalized total and concentration dynamic structure factors (6). The left frame of Fig. 8 gives evidence that the main contribution to $S_{tt}(k,\omega)$ comes from structural relaxation and only small contribution is from acoustic excitations in the long-wavelength region, that explains the shape of total dynamic structure factor in Fig. 1. In contrast to total dynamic structure factors the concentration one $S_{cc}(k,\omega)$ contains a side peak from high-frequency collective excitations. For analysis of contributions to concentration dynamic structure factors of molten salts one can make use of analytical expression for the long-wavelength limit[19]

$$A^{cond}_{cc}(k\to 0)\to 1-\Delta$$
$$B^{opt}_{cc}(k\to 0)\to \Delta, \qquad (7)$$

where the parameter Δ depends on normalized second frequency moment of $S_{cc}(k,\omega)$ as well as on $d_{cond}(k\to 0)$, frequency $\omega_{opt}(k\to 0)$, and damping of optic-like modes $\sigma_{opt}(k\to 0)$.[19] In comparison with the rigid ion case the damping of optic-like modes becomes almost two times larger, that results in their smaller contribution to $S_{cc}(k,\omega)$, and according to (7) the corresponding contribution from the mode $d_{cond}(k)$ is increasing. Indeed this can be seen from comparison of results shown in Figs. 8 and 9, where the mode contributions to $S_{tt}(k,\omega)$ and $S_{cc}(k,\omega)$ obtained for rigid ion model are presented. The wave-number dependence of main contributions to $S_{tt}(k,\omega)$ from both simulations is almost the same. However for $S_{cc}(k,\omega)$ the polarization effects essentially change the relative strength of contributions from optic modes and relaxation process $d_2(k)$. Indeed, in agreement with the dependence of $d_2(k)$ on ε_∞ the mode contribution of more slow relaxing mode $d_2(k)$ to $S_{cc}(k,\omega)$ is much stronger than for the case of rigid ions (right frame in Fig. 9). This explains the different amplitude of the central peak of $S_{cc}(k,\omega)$ from *ab initio* and RI simulations (see right frame in Fig. 2) and observed shoulder from optic modes in *ab initio*-derived $S_{cc}(k,\omega)$ and well-defined side peak from optic modes in rigid ion model.

In Fig. 10 the wave-number dependent mode contributions are shown for partial Li-Li and Br-Br dynamic structure factors. It is seen that in the region $k > 0.5$ Å^{-1} different types of collective excitations contribute to the partial dynamic structure factors. The partial dynamic structure factor of light component $S_{\mathrm{LiLi}}(k,\omega)$ in this wave-number range contains the contribution from the high-frequency branch whereas the contribution from the low-frequency branch is practically very close to zero. The opposite situation is observed in the case of the partial dynamic structure factor of heavy component $S_{\mathrm{BrBr}}(k,\omega)$. This fact reflects the existence of "partial" dynamics in the disparate mass binary liquids:[11,25] the higher is the mass ratio the narrower is the long-wavelength region with typical hydrodynamic behaviour of collective modes and right beyond the hydrodynamic regime begins the region of "partial" dynamics. For the small wave numbers we observe for $S_{\mathrm{LiLi}}(k,\omega)$ the tendency for increasing of contribution from the low-frequency mode and decreasing (down to complete vanishing in the $k\to 0$ limit) of the contribution from the non-hydrodynamic high-frequency optic mode. This is exactly the same crossover of mode contributions observed in the disparate-mass metallic liquid alloys Li_4Pb[11] and Li_4Tl[12] by approaching the hydrodynamic regime. It is clear, that in the $k\to 0$ limit the only contribution to the side peaks of different dynamic structure factors can come from the hydrodynamic acoustic modes.

IV. CONCLUSIONS

We performed the *ab initio* study of collective excitations in a disparate-mass molten salt LiBr and estimated the main mode contributions to various dynamic structure factors. The main conclusions of this study are listed as follows:

- we calculated by a combination of *ab initio* molecular dynamics and a six-variable (and four-variable for transverse case) GCM dynamic model the dispersion and damping of the low- and high-frequency branches of collective excitations in a wide region of wave numbers;
- we observed the effect of softening of the longitudinal optic branch due to polarization effects. The gap between LO and TO long-wavelength excitations in molten LiBr was reduced by ~1.82 times that is in agreement with the suggested in[49] renormalization of the LO-TO gap by $\sqrt{\varepsilon_\infty}$ times. The value of the high-frequency dielectric permittivity ε_∞ was estimated for

LiBr in this study as equal to 3.32 that is in good agreement with the high-frequency dielectric permittivity of LiBr crystals;[39]

- we were able to calculate from *ab initio* simulations the electron-ion static structure factors and observed the different sign of $S_{el-ion}(k)$ in the region of main peak location of $S_{cc}(k)$. The comparison of numerical results with analytical asymptotes[40,41] showed perfect agreement in the long-wavelength region;
- similar wave-number dependent mode contributions to total dynamic structure factors $S_{tt}(k, \omega)$ were observed from *ab initio* and classical rigid ion simulations. For the concentration dynamic structure factor $S_{cc}(k, \omega)$ the polarization effects essentially change the mode contributions in comparison with the RI case making stronger the contribution from relaxation mode $d_{cond}(k)$ and decreasing the contribution from optic modes;
- the wave-number dependent mode contributions to partial dynamic structure factor of light component $S_{\mathrm{LiLi}}(k, \omega)$ were obtained very similar as for the previously studied mode contributions in the "fast sound" liquid alloys Li_4Pb[11] and Li_4Tl[12] that gives evidence of the same type of crossover in mode contributions by approaching the hydrodynamic regime.

ACKNOWLEDGMENTS

This study was partially supported by the NASU Program "Fundamental properties of matter in a wide range of spatial and time scales" and Grid-project No. 0112U003269. The calculations have been performed using the *ab initio* total-energy and molecular dynamics program VASP (Vienna *ab initio* simulation program) developed at the Institute für Materialphysik of the Universität Wien.[50–52]

[1]W. Montfrooij and I. De Schepper, *Excitations in Simple Liquids, Liquid Metals and Superfluids* (Oxford University Press, New York, 2010).
[2]J. Bosse, G. Jacucci, M. Ronchetti, and W. Schirmacher, Phys. Rev. Lett. **57**, 3277 (1986).
[3]P. H. K. de Jong, P. Verkerk, C. F. de Vroege, L. A. de Graaf, W. S. Howells, and S. M. Bennington, J. Phys.: Condens. Matter **6**, L681 (1994).
[4]P. Westerhuijs, W. Montfrooij, L. A. de Graaf, and I. M. de Schepper, Phys. Rev. A **45**, 3749 (1992).
[5]E. Enciso, N. G. Almarza, M. A. Gonzalez, F. J. Bermejo, R. Fernandez-Perea, and F. Bresme, Phys. Rev. Lett. **81**, 4432 (1998).
[6]Ya. Chushak, T. Bryk, A. Baumketner, G. Kahl, and J. Hafner, Phys. Chem. Liq. **32**, 87 (1996).
[7]N. Anento, L. E. Gonzalez, D. J. Gonzalez, Ya. Chushak, and A. Baumketner, Phys. Rev. E **70**, 041201 (2004).
[8]I. M. deSchepper, E. G. D. Cohen, C. Bruin, J. C. van Rijs, W. Montfrooij, and L. A. de Graaf, Phys. Rev. A **38**, 271 (1988).
[9]I. M. Mryglod, I. P. Omelyan, and M. V. Tokarchuk, Mol. Phys. **84**, 235 (1995).
[10]T. Bryk, I. Mryglod, and G. Kahl, Phys. Rev. E **56**, 2903 (1997).
[11]T. Bryk and I. Mryglod, J. Phys.: Condens. Matter **17**, 413 (2005).
[12]T. Bryk and J.-F. Wax, Phys. Rev. B **80**, 184206 (2009).
[13]N. H. March and M. P. Tosi, *Coulomb Liquids* (Academic, London/New York, 1984).
[14]J.-P. Hansen and I. R. McDonald, *Theory of Simple Liquids* (Academic, London, 1986).
[15]T. Bryk, Eur. Phys. J. Spec. Top. **196**, 65 (2011).
[16]T. Bryk and I. Mryglod, Phys. Rev. E **64**, 032202 (2001).
[17]P. V. Giaquinta, M. Parrinello, and M. P. Tosi, Phys. Chem. Liq. **5**, 305 (1976).
[18]P. V. Giaquinta, M. Parrinello, and M. P. Tosi, J. Phys. C: Solid State Phys. **8**, L501 (1975).
[19]T. Bryk and I. Mryglod, J. Phys.: Condens. Matter **16**, L463 (2004).
[20]J.-P. Hansen and I. R. McDonald, Phys. Rev. A **11**, 2111 (1975).
[21]G. Ciccotti, G. Jacucci, and I. R. McDonald, Phys. Rev. A **13**, 426 (1976).
[22]T. Bryk and I. Mryglod, Phys. Lett. A **261**, 349 (1999).
[23]S. Hosokawa, M. Inui, T. Bryk, I. Mryglod, F. Demmel, W.-C. Pilgrim, Y. Kajihara, K. Matsuda, M. Yao, Y. Ohmasa, S. Tsutsui, and A. Q. R. Baron, Detection of collective optic excitations in molten NaI, Abstracts, LAM-14, Rome, Italy (2010), p. 240.
[24]T. Bryk and I. Mryglod, J. Phys.: Condens. Matter **12**, 6063 (2000).
[25]T. Bryk and I. Mryglod, J. Phys.: Condens. Matter **14**, L445 (2002).
[26]F. Lantelme, P. Turq, and P. Schofield, J. Chem. Phys. **67**, 3869 (1977).
[27]O. Alcaraz and J. Trullas, J. Chem. Phys. **113**, 10635 (2000).
[28]T. Bryk and I. Mryglod, Phys. Rev. B **71**, 132202 (2005).
[29]T. Bryk and I. Mryglod, Chem. Phys. Lett. **466**, 56 (2008).
[30]T. Bryk and I. Mryglod, Phys. Rev. B **79**, 184206 (2009).
[31]T. Bryk and I. Mryglod, Int. J. Quantum Chem. **110**, 38 (2010).
[32]B. Markiv, A. Vasylenko, and M. Tokarchuk, J. Chem. Phys. **136**, 234502 (2012).
[33]P. V. Giaquinta, M. Parrinello, W. Bouché, and M. P. Tosi, Lett. Nuovo Cimento **19**, 215 (1977).
[34]P. E. Blöchl, Phys. Rev. B **50**, 17953 (1994).
[35]G. Kresse and D. Joubert, Phys. Rev. B **59**, 1758 (1999).
[36]J. P. Perdew, K. Burke, and M. Ernzerhof, Phys. Rev. Lett. **77**, 3865 (1996).
[37]M. Wilson, P. A. Madden, and B. J. Costa-Cabral, J. Phys. Chem. **100**, 1227 (1996).
[38]T. Bryk and I. Mryglod, Phys. Rev. E **63**, 051202 (2001).
[39]G. Lucovsky, R. M. Martin, and E. Burstein, Phys. Rev. B **4**, 1367 (1971).
[40]N. H. March, M. P. Tosi, and A. B. Bhatia, J. Phys. C **6**, L59 (1973).
[41]M. P. Tosi and N. H. March, Nuovo Cimento **15**, 308 (1973).
[42]C. Massobrio and A. Pasquarello, Phys. Rev. B **68**, 020201(R) (2003).
[43]C. Massobrio, M. Celino, and A. Pasquarello, Phys. Rev. B **70**, 174202 (2004).
[44]I. Klevets and T. Bryk (unpublished).
[45]T. Bryk, I. Mryglod, T. Scopigno, G. Ruocco, F. Gorelli, and M. Santoro, J. Chem. Phys. **133**, 024502 (2010).
[46]F. Bencivenga and A. Cunsolo, J. Chem. Phys. **136**, 114508 (2012).
[47]A. Cunsolo, J. Phys.: Condens. Matter **24**, 375104 (2012).
[48]T. Bryk and I. Mryglod, Condens. Matter Phys. **11**, 139 (2008).
[49]K. F. O'Sullivan and P. A. Madden, J. Phys.: Condens. Matter **3**, 8751 (1991).
[50]G. Kresse and J. Hafner, Phys. Rev. B **47**, 558 (1993); **49**, 14251 (1994).
[51]G. Kresse and J. Furthmüller, Comput. Mater. Sci. **6**, 15 (1996).
[52]G. Kresse and J. Furthmüller, Phys. Rev. B **54**, 11169 (1996).